International Journal of Mechanical, Industrial and Aerospace Sciences
ISSN: 2517-9950
Vol:10, No:2, 2016

Effects of Roughness on Forward Facing Step in an Open Channel

S. M. Rifat, André L. Marchildon, Mark F. Tachie

***Abstract*—**Experiments were performed to investigate the effects of roughness on the reattachment and redevelopment regions over a 12 mm forward facing step (FFS) in an open channel flow. The experiments were performed over an upstream smooth wall and a smooth FFS, an upstream wall coated with sandpaper 36 grit and a smooth FFS and an upstream rough wall produced from sandpaper 36 grit and a FFS coated with sandpaper 36 grit. To investigate only the wall roughness effects, Reynolds number, Froude number, aspect ratio and blockage ratio were kept constant. Upstream profiles showed reduced streamwise mean velocities close to the rough wall compared to the smooth wall, but the turbulence level was increased by upstream wall roughness. The reattachment length for the smooth-smooth wall experiment was 1.78h; however, when it is replaced with rough-smooth wall the reattachment length decreased to 1.53h. It was observed that the upstream roughness increased the physical size of contours of maximum turbulence level; however, the downstream roughness decreased both the size and magnitude of contours in the vicinity of the leading edge of the step. Quadrant analysis was performed to investigate the dominant Reynolds shear stress contribution in the recirculation region. The Reynolds shear stress and turbulent kinetic energy profiles after the reattachment showed slower recovery compared to the streamwise mean velocity, however all the profiles fairly collapse on their corresponding upstream profiles at x/h = 60. It was concluded that to obtain a complete collapse several more streamwise distances would be required.

***Keywords*—**Forward facing step, open channel, separated and reattached turbulent flows, wall roughness.

I. Introduction

OVER the past decades, separated and reattached flows have received significant research attention due to their diverse engineering, environmental and industrial applications. Some of these applications are pipe flows, combustors, turbine blades, airfoils and wind turbines. For a fluid-thermal system, the phenomenon of flow separation and reattachment can result in a variety of problems including flow-induced structural vibration and significant reduction in efficiency. Numerous numerical and experimental investigations have been performed to understand the characteristics of separated and reattached flows produced from fences, ribs, backward facing step (BFS) and forward facing step (FFS). However, only a few studies examined the effects of upstream roughness effects on the separation and reattachment process, and no system investigation of both upstream and downstream roughness effects on redevelopment after flow reattachment has been reported yet. Thus our understanding of wall roughness on separation and flow development after the reattachment is incomplete. Therefore, the motivation of the present study is to investigate the effects of upstream and downstream roughness on reattachment and redevelopment of a FFS immersed in an open channel turbulent flow.

A schematic diagram of the flow regions of a FFS is shown in Fig. 1 together with the Cartesian coordinate system adopted. The x-coordinate is aligned with the streamwise direction and the y-coordinate is aligned with the wall-normal direction. The flow field over a FFS can be divided into three distinct regions: an upstream recirculation region before the step, a primary recirculation region on top of the step and a redevelopment region after the reattachment. The upstream mean freestream velocity is denoted by U_e, the boundary layer thickness is δ and the height of the step is denoted by h. Due to the adverse pressure gradient caused by the step, the flow first separates and then reattaches on the front wall of the step. The height and length of this separation and reattachment are denoted by h_u and l_r, respectively. Subsequently, the flow separates at the leading edge of the step and reattaches after some distance on top of the wall of the step. This distance is defined as the reattachment length, L_r and the maximum height of this recirculation bubble is denoted by h_d. After the reattachment, a new shear layer forms and develops into a new boundary layer.

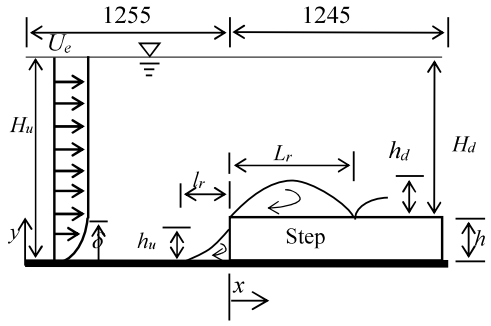

Fig. 1 Different regions of FFS and nomenclature

The flow characteristics over a FFS are found to be affected by different dimensional parameters, primarily the geometry and initial boundary layer conditions such as aspect ratio, $AR = W/h$ (where W is the width of the channel), blockage ratio, $BR = h/H_u$ (where H_u is the upstream channel height), upstream boundary layer thickness to step height ratio, δ/h,

S. M. Rifat is a graduate student in Mechanical Engineering Department at the University of Manitoba, Winnipeg, MB R3T 5V6, Canada.
A. L. Marchildon is an undergraduate mechanical engineering student at the University of Manitoba, Winnipeg, MB R3T 5V6, Canada.
M. F. Tachie is a professor in Mechanical Engineering Department at the University of Manitoba, Winnipeg, MB R3T 5V6, Canada (corresponding author, phone: +12044749589, fax: +12042757507, e-mail: mark.tachie@umanitoba.ca).

Reynolds number based on step height and freestream velocity, $Re_h = U_e h/\nu$ (where ν is the kinematic viscosity), upstream turbulence intensity (T_u) and equivalent sand grain roughness Reynolds number (k_s^+). For an open channel flow, Froude number based on upstream channel height, $Fr_H = U_e/\sqrt{(gH_u)}$ is also a very important parameter on which the flow characteristics depend. References [1], [2] investigated the effects of positive and negative roughness slopes on top of the FFS. They conducted their study in a wind tunnel using a particle image velocimetry (PIV) at $Re_h = 3450$ and $\delta/h = 8$. They observed that the upstream recirculation region was little affected by the surface topographies on top of the step but the downstream recirculation region was sensitive to the positive and negative roughness slopes. For example, a recirculation bubble was not observed for the positive slope, however for a negative slope, the recirculation bubble was similar to that of a smooth FFS although its centre location was slightly shifted downstream. The authors concluded that the rough surface conditions on top of the FFS weakened the separated flow but its effects might be confined within $2h$-$3h$ downstream of the leading edge of the step. Reference [3] is another study in which roughness effect on a FFS was investigated. In this study, PIV measurements were performed to examine the effects of upstream roughness on a smooth FFS in a closed channel. They used a fixed blockage ratio of 0.2 but varied the Reynolds numbers from 2040 to 9130. They found a threshold value for reattachment length, $Re_h > 5800$ for the smooth wall and $Re_h > 4010$ for the rough wall, beyond which the reattachment length is independent of the Reynolds number. It was also observed that before these threshold values of Re_h, the reattachment length for smooth wall increased monotonically but decreased in the case of rough wall. Upstream roughness was observed to reduce the mean reattachment lengths and but enhanced the turbulent kinetic energy in the recirculation bubble and early development. Quadrant decomposition analysis was performed to provide insight into the Reynolds shear stress producing events; and the results indicate that upstream roughness decreased the ejections and sweeps events but the inward and outward interaction motions were independent of upstream roughness.

As noted earlier, only a few studies were conducted to examine the effects of upstream roughness on flow separation, reattachment and the dynamics in the early redevelopment region. A few studies were also undertaken in the past to examine the relaxation of the boundary layer far downstream of the leading edge of the step. Reference [4] is an example in this regard. They performed their experiment in an open channel flume and velocity measurements were made using a single-component fiber-optics Laser-Doppler Anemometer (LDA). They found that the structure of the flow was reasonably self-similar to the corresponding upstream structure at $x/h \geq 50$. The viscous sublayer was insensitive to the imposed disturbance or recovery process, and the skin friction coefficient was invariant with downstream location at $x/h \geq 50$. They observed two peaks in the turbulence intensity profiles; the outer peak was speculated to be an artifact of the complex shear layer in the recirculation region. They concluded that the turbulence statistics recover satisfactorily at $x/h = 100$ if self-similarity was used as a criterion, otherwise, in some of the flows complete recovery might not be achieved.

Reference [5] examined the mean and turbulent fields in separated and redeveloped flow over square, rectangular and semicircular blocks in an open channel. They observed the variation of the Reynolds stress along the dividing streamlines in the context of vortex stretching, longitudinal strain rate and wall damping. They concluded that parameters such as skin friction coefficient, momentum thickness, shape factor and Clauser shape parameter strongly depend on geometry over the first $25h$-$50h$ downstream of reattachment. It was noted that a very long redevelopment length will be required for the integral parameters and the Reynolds stresses to collapse onto their corresponding upstream values.

The objective of the present study is to investigate the effects of upstream and downstream roughness on characteristics of the reattachment and redevelopment regions over a FFS placed in a shallow open channel turbulent flow. A series of experiments were performed in which the Reynolds number, Froude number, blockage ratio and channel aspect ratio were all kept constant but the upstream and downstream wall conditions were varied from a reference smooth wall to a different rough wall made from sandpaper 36 grit. Three different test cases are investigated in this paper; an upstream smooth wall and a smooth FFS, an upstream wall coated with sandpaper 36 grit and a smooth FFS, and an upstream rough wall produced from sandpaper 36 grit and a FFS coated with sandpaper 36 grit. A PIV technique was used to conduct detailed velocity measurements, and the velocity data were post-processed to characterise how changes in the upstream and downstream wall roughness affect the separation bubbles and flow redevelopments, and also the mean velocity and higher order turbulence statistics in the separation and reattachment regions. Quadrant analysis was used to quantify the contribution of ejections and sweeps as well as inward and outwards interaction motions to the Reynolds shear stress.

II. Experimental Procedure

A schematic of the test section is shown in Fig. 1. The experiments were performed in a recirculating open channel of 2500 mm length and 186 mm inner width. The test section was made with transparent acrylic plates for easier optical access. The FFS used to induce the flow separation in this study was made of acrylic plates of height, $h = 12$ mm. The FFS was positioned 1255 mm downstream from the inlet of the channel and spanned about 1245 mm to the end of the channel. To ensure that the flow becomes fully developed before interaction with the step, a 3.5 mm square trip, spanning the whole width of the channel was placed on the inlet wall. The water depth was 60 mm prior to the step in the channel. The aspect ratio ($AR = W/h$) was 15.5 which is larger than a threshold value of 10 required to make the flow two dimensional at the mid span of the channel [6], [7]. The blockage ratio in this study was (h/H_u) = 0.2. The Reynolds numbers based on the upstream water height and step height

were, respectively, $Re_H \approx 17000$ and $Re_h \approx 3400$, which were all kept constant throughout the experiments. The Froude number based on upstream water height was kept constant at $Fr \approx 0.35$ which ensure a fairly calm water surface.

As noted earlier, three different cases of upstream and downstream roughness were investigated. The smooth upstream and downstream walls investigated (hereafter referred to as SM-SM) was made of 6 ± 0.1 mm thick acrylic plates. The rough wall in the rough upstream and smooth downstream case was made by gluing 1.5 mm thick roughness elements consisting of sandpaper 36 grit (hereafter referred to as SP-SM) onto 4.5 mm thick acrylic plates resulting in a combined height of 6 ± 0.1 mm. The rough walls in rough upstream and downstream case were coated with the same roughness elements (hereafter referred to as SP-SP) resulting in a combined height of 6 ± 0.1 mm. To obtain the topographical information of the roughness elements, a Veeco Wyco NT9100 optical profilometer was used. This particular profilometer uses white light interferometry with sub-micron vertical accuracy. The surface statistics for the sandpaper 36 grit are summarized in Table I; where kt is the average of ten maximum peak-to-trough roughness heights, the root-mean-square roughness height is denoted by k_{rms}, Sk and Ku are the skewness and flatness of the roughness probability density function, respectively. The equivalent sand grain roughness of the roughness elements was determined using (1) proposed by [8]:

$$k_s = 4.43 k_{rms} \left(1 + Sk\right)^{1.37} \quad (1)$$

TABLE I
SURFACE TOPOGRAPHY OF SANDPAPER 36 GRIT

k_t (mm)	k_s (mm)	k_{rms} (mm)	Sk	Ku
1.12	1.37	0.16	0.61	3.23

A planar particle image velocimetry (PIV) was used to conduct detailed velocity measurements in x-y plane situated in the mid span of the open water channel. The flow was seeded with 10 μm fluorescent tracer particles and a double-pulsed Nd:YAG laser (120 mJ/pulse) was used to illuminate the flow. The scattered light from the particles were captured by a 12-bit charge couple device (CCD) camera with 2048 × 2048 pixel array and 7.4 pixel pitch. The camera was equipped with an orange filter with band pass wavelength of 570 nm which improves the quality of the velocity vectors close to the walls by reducing the glare. The field of view was set to 70 mm × 70 mm. Detailed velocity measurements were performed in several planes; an upstream plane PA that spanned from -25h to -19.2h was used to characterize the approach boundary layer, P0 and P1 planes were chosen to capture the flow fields within the separation and reattachment regions which extent up to 4.3h. In order to observe the behaviour of flow in the redevelopment regions, velocity measurements were performed in six different planes up to 60h streamwise extent. Following a thorough convergence test, a sample size of 5000 instantaneous image pairs was acquired and the adaptive correlation option in DynamicStudio version 4.10 (Dantec Dynamics Inc.) was used to post process the data. An interrogation area of 32 pixels × 32 pixels with 50% overlap was used in the adaptive correlation. The spacing between adjacent vectors was 0.046h in both x and y direction. The time between image pairs and the size of the integration area were chosen to ensure that the average displacement of particles was less than one quarter of the length of the integration area.

To reduce the bias and precision errors associated with the PIV system, precautionary guidelines and advanced evaluation algorithms described by [9] were used. Using the procedure recommended by [10], the uncertainty at 95% confidence level in the mean velocities was 1.4% of the streamwise velocity. The uncertainty for the turbulence intensity and Reynolds shear stress was 2% and 2.8% respectively.

III. RESULTS AND DISCUSSION

A. Upstream Approach Boundary Layer

The velocity measurements performed in the upstream plane of the reference smooth wall (SM-SM) and rough walls (SP-SM and SP-SP) were analyzed to properly characterize the state of the boundary layers prior to encountering the FFS. The upstream walls for the latter two cases were made of the same roughness type (i.e., sandpaper 36 grit), so only one case will be used to compare the upstream conditions with the SM-SM case. To examine the initial condition of the approach flow, profiles of streamwise mean velocity were obtained at x/h = -22 over both SM and SP walls. The distribution of the streamwise mean velocity profiles showed that the profiles over the rough walls are less uniform than over the smooth wall which can be attributed to the higher mass and momentum deficit as well as the higher drag produced by the wall roughness. At $y = h$, the mean streamwise velocity is $0.762U_e$ over the smooth wall but reduced to $0.747U_e$ over the rough wall. This comparison clearly indicates that wall roughness reduced the approach velocity albeit marginally. To observe the effects of upstream roughness in the approach flow condition more closely, the boundary layer shape factor ($H = \delta^*/\theta$) and Reynolds number based on the momentum thickness ($R_{e\theta}$) were calculated and the results are summarized in Table II. The shape factor was increased by the wall roughness. The Clauser plot technique was used to determine the friction velocities, U_τ and skin friction coefficient, C_f which are also presented in Table II. It can also be seen from the results that the roughness condition of SP is in the transitional rough regime ($k_s^+ < 70$) which is why the increase of shape factor and skin friction coefficient in rough wall is not very large compared to their smooth wall counterparts. Wall roughness was also observed to increase both the streamwise and wall-normal turbulence intensities particularly in the immediate vicinity of the wall. For instance, at the same height of the step ($y = h$), the streamwise turbulence intensities for the smooth and rough wall were $0.065U_e$ and $0.074U_e$ respectively; which is a clear indication that the rough wall increased the turbulence intensity by 14% compared to the corresponding smooth wall.

TABLE II
UPSTREAM BOUNDARY LAYER PARAMETERS AND REATTACHMENT LENGTHS

Wall topography	U_e (mm)	Re_θ	H	C_f	k_s^+	L_r/h	h_d/h
SM	0.267	1930	1.33	0.0040	-	1.78	0.16
SP	0.272	2000	1.39	0.0042	13	1.53	0.12

B.Separated and Reattached Region

The streamwise and wall-normal mean velocities, turbulence intensities and Reynolds shear stress are used to examine the effects of upstream roughness on the recirculation bubble. Fig. 2 shows the contour plots of streamwise mean velocity in the separated and reattached region for the three test cases. The physical size of the recirculation bubble is defined as the region enclosed by the $U/U_e = 0$ contour level and the top surface of the step. The upstream recirculation region or secondary recirculation bubble was affected by the upstream roughness. Changing the upstream wall from a smooth wall to a rough wall increased the height of the secondary reattachment; it was closer to the leading edge of the step for the rough wall cases than the smooth wall case. Similar to the secondary recirculation bubble, the downstream recirculation region or primary recirculation region is found to be sensitive to roughness topographies. The mean reattachment length over step height, L_r/h and the mean reattachment height over step height, h_d/h are decreased for SP-SP compared to SM-SM due to the relatively larger momentum deficit and higher turbulence produced by wall roughness. Specifically, SP-SM showed a decrease of 14% and 25% in L_r/h and h_d/h respectively compared to the corresponding smooth wall values. SP-SP did not show any distinct primary recirculation bubble. Similar observation was reported in [2], and a probable reason for this is that the average height of the irregular roughness elements on top of the step is of the same size as the height of the recirculation bubble thereby disrupted a well-defined recirculation region to be formed.

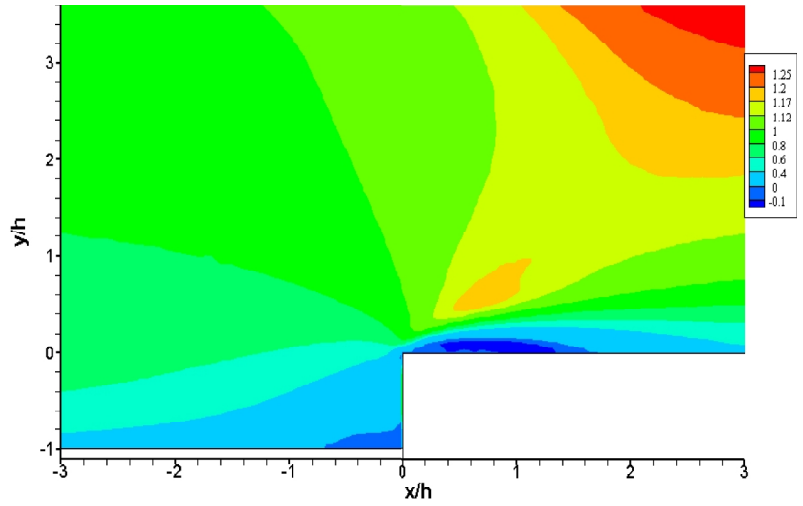

(a)

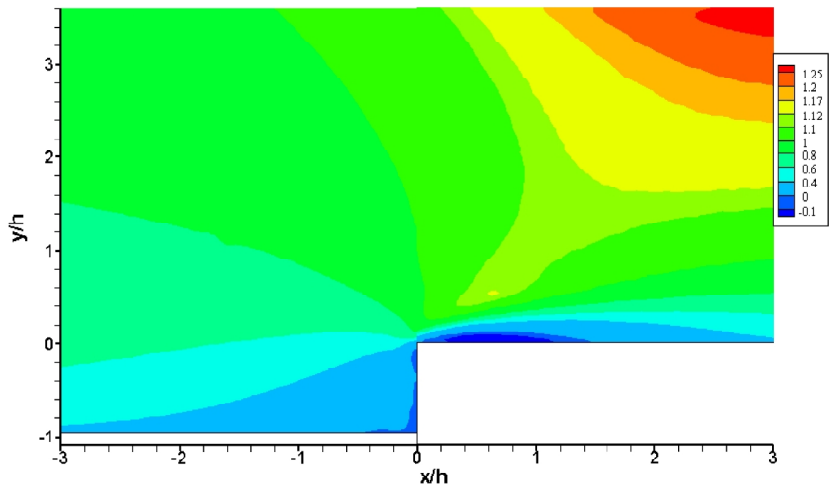

(b)

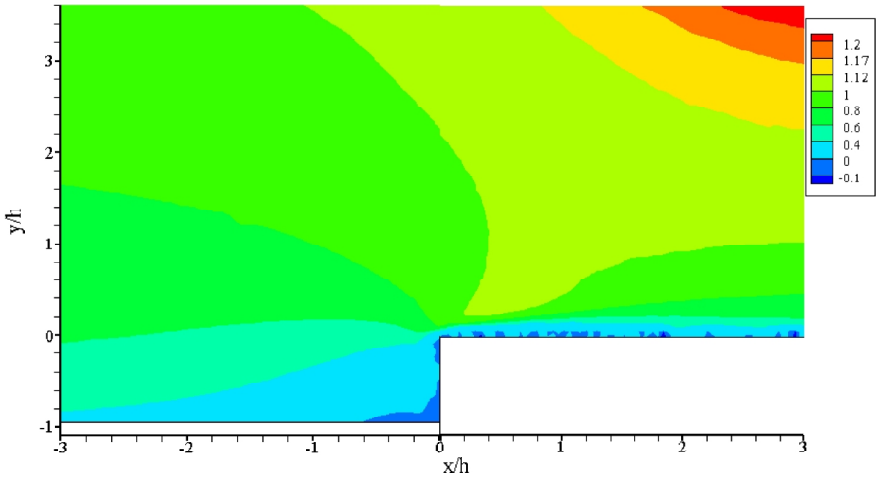

(c)

Fig. 2 Contour plots of streamwise mean velocity in the recirculation region for (a) SM-SM, (b) SP-SM and (c) SP-SP

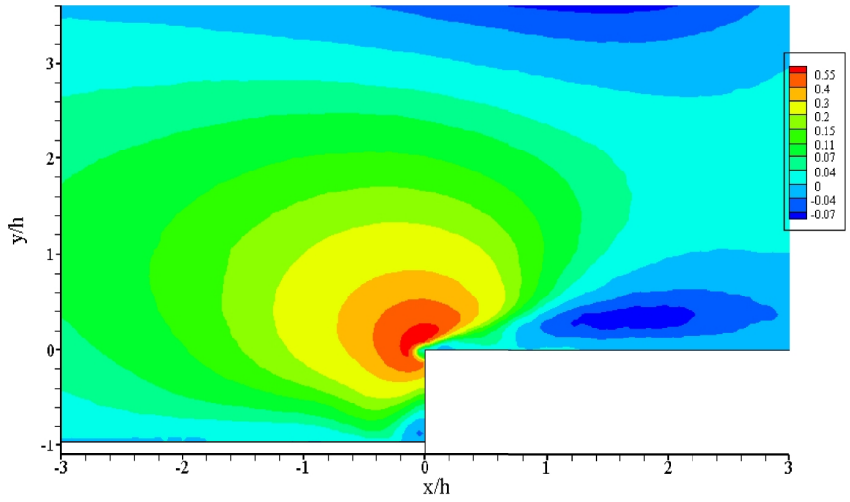

(a)

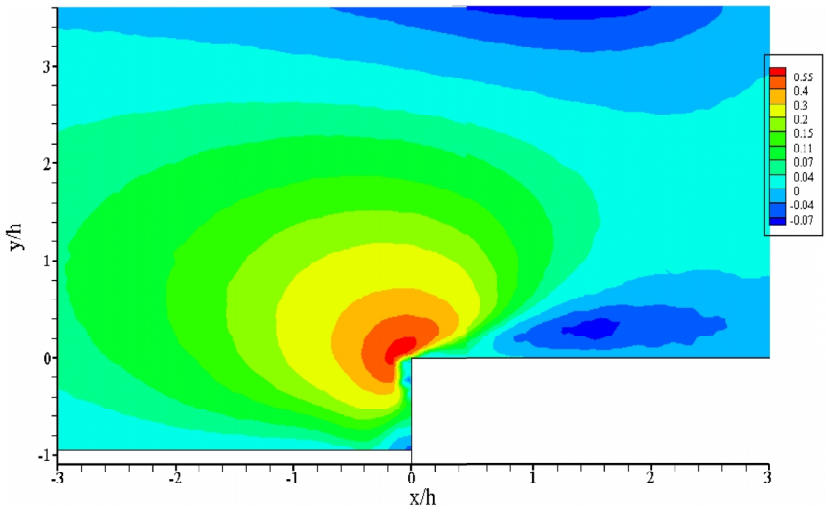

(b)

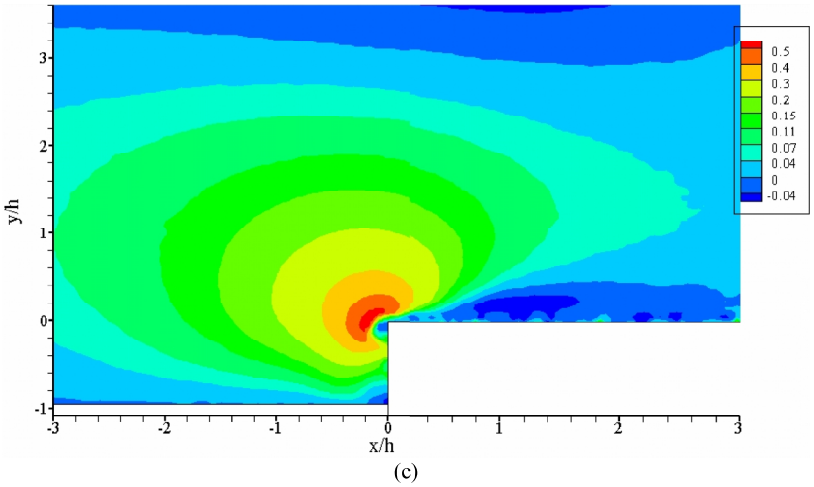

Fig. 3 Contour plots of wall-normal mean velocity in the recirculation region for (a) SM-SM, (b) SP-SM and (c) SP-SP

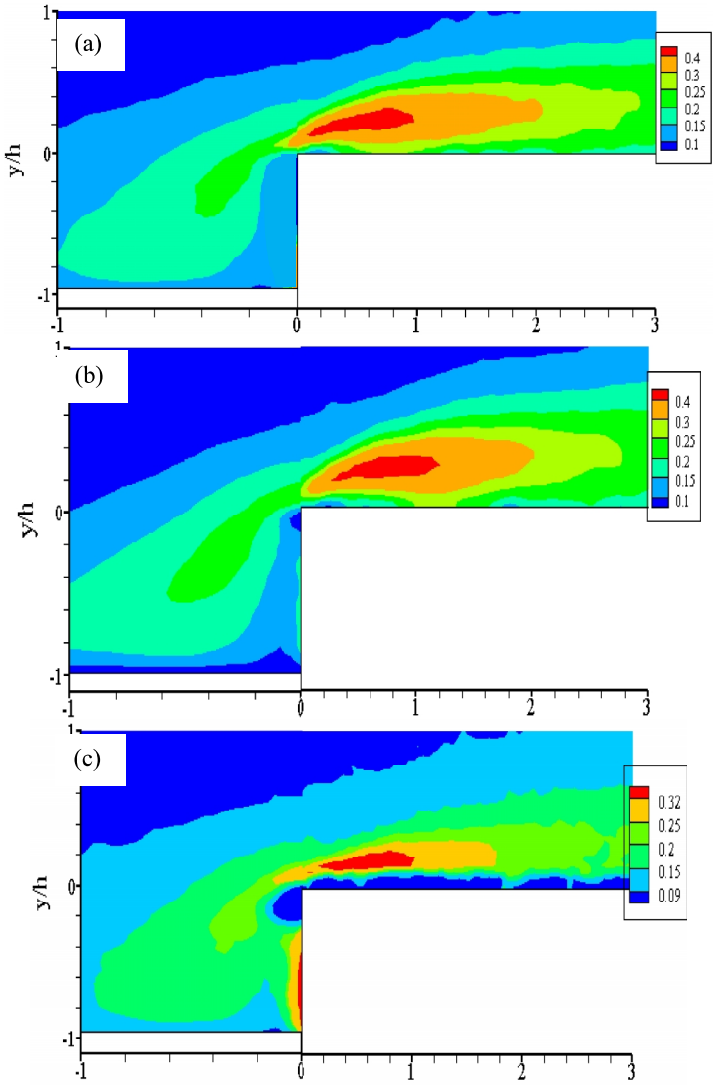

Fig. 4 Contour plots of streamwise turbulence intensity in the recirculation region for (a) SM-SM, (b) SP-SM and (c) SP-SP

Due to the relatively higher momentum fluid over the smooth wall compared to the rough wall, it is not surprising to observe high local streamwise velocities in the vicinity of the leading edge of the step. For example, SM-SM has a higher local velocity of $1.17U_e$ compared to $1.12U_e$ for SP-SM. The higher momentum fluid over the smooth wall caused the flow to deflect more aggressively into the separated shear layer over the step compared to the reduced momentum fluid over the upstream rough wall. No distinct local maxima were observed close to the step leading edge when the smooth step is replaced by a step roughened by sand paper, i.e., SP-SP case.

The contours of wall-normal mean velocities are examined in Fig. 3. In the vicinity of the leading edge of the step, the flow is deflected due to the presence of the step. This creates a high positive wall-normal velocity, $0.55U_e$ for SM-SM and SP-SM and $0.50U_e$ for SP-SP in that region, but as the roughness increases the physical size of this contour level decreases. The decrease in the size of the contour levels due to the roughness indicates that for the upstream rough wall, the ability of the flow to permeate into the outer high-speed flow by the low momentum fluid is less than observed for the smooth upstream. After the deflection, when the flow is coming downwards, it entrains the freestream fluid into the separated shear layer which causes the negative wall-normal velocities to occur. The maximum negative wall-normal velocity was reduced both in size and magnitude when SM-SM is replaced by SP-SM and SP-SP. For SM-SM and SP-SM it is $0.07U_e$ and for SP-SP it is $0.04U_e$. Similar observations were reported in [11].

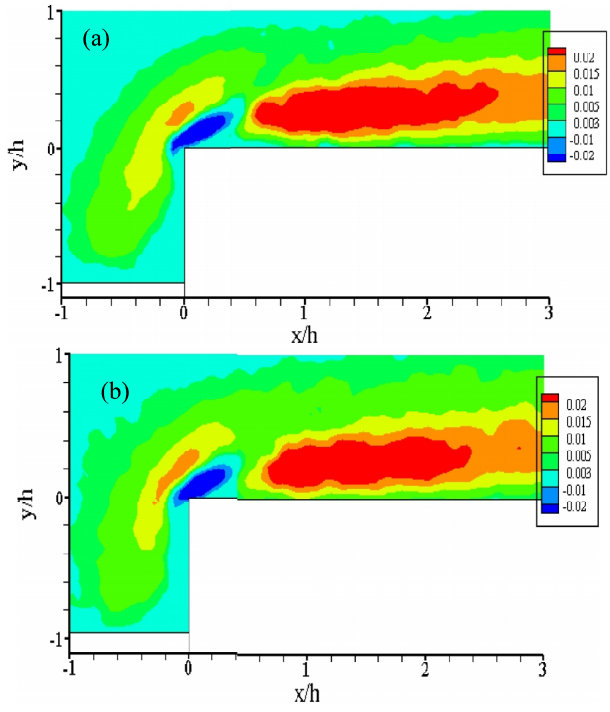

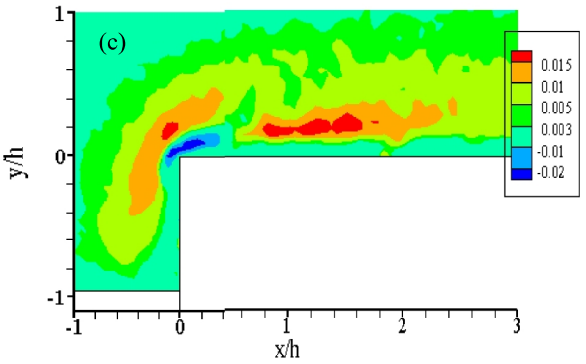

Fig. 5 Contour plots of Reynolds shear stress in the recirculation region for (a) SM-SM, (b) SP-SM and (c) SP-SP

Fig. 4 shows the contour plots of streamwise turbulence intensity in the recirculation region. The maximum turbulence intensity for SM-SM and SP-SP is $0.4U_e$ whereas for SP-SP it is $0.32U_e$. The maximum contour level is observed just after the leading edge of the step. Although the upstream roughness increases the size of the maximum contour level, the presence of downstream roughness decreases the magnitude and squeezed the size of the maximum contour level in the vicinity of the leading edge.

Fig. 5 shows the contour plots of Reynolds shear stress in the recirculation region. In the immediate vicinity of the step, maximum negative $<-u'v'>$ can be observed and after about one step height from the leading edge of the step the maximum positive $<-u'v'>$ is observed. The position of the negative and positive $<-u'v'>$ coincides with the position of positive and negative wall-normal mean velocity contour plots which can be related to the transport of low and high momentum fluid upward and toward the wall respectively. The magnitude of both the maximum negative and positive $<-u'v'>$ was 0.02Ue for both SM-SM and SP-SM and 0.015Ue for SP-SP. Changing the upstream wall condition from smooth to rough, the size of both the maximum positive and negative $<-u'v'>$ contour levels decreased. For SP-SP, the downstream rough wall decreased the physical size of the maximum positive $<-u'v'>$ contour level even more than SP-SM.

One dimensional profiles of streamwise mean velocity, Reynolds shear stress and turbulent kinetic energy at different x/h locations near and far downstream of the step will be discussed in this section. These profiles are obtained at selected locations (x/h = -22, 0.5, 5, 10, 30 and 60) which include locations in the upstream region, early redevelopment region and far downstream region for each case. All the profiles are normalized by the local maximum velocity U_m. Ideally in a separated and reattached flow over FFS, the flow structures after the reattachment should be self-similar to the respective upstream profiles. Therefore, the downstream profiles are compared to the corresponding upstream profiles to examine how the flow redevelops to their upstream values. To examine when the profiles start becoming self-similar, the upstream smooth profiles are super-imposed at every x/h location for both SM-SM and SP-SM cases as they both have the same smooth downstream surface condition. For SP-SP

case, as the downstream surface is rough, rough upstream profiles are imposed at every location.

Fig. 6 shows the streamwise mean velocity profiles. The effects of upstream wall roughness have more noticeable effect on streamwise velocity profiles close to the wall than in the region away from the wall. In all the test cases, the streamwise mean velocity profiles close to the wall slowly recovered from the disturbance caused by the severe adverse pressure gradient of the step. Due to the recirculation close to the wall, there is a negative streamwise velocity or backflow at x/h = 0.5 for both SM-SM and SP-SM, but as there is no recirculation for SP-SP, no backflow at this location was observed. The maximum backflow for SM-SM and SP-SM was $0.14U_m$ and $0.21U_m$.

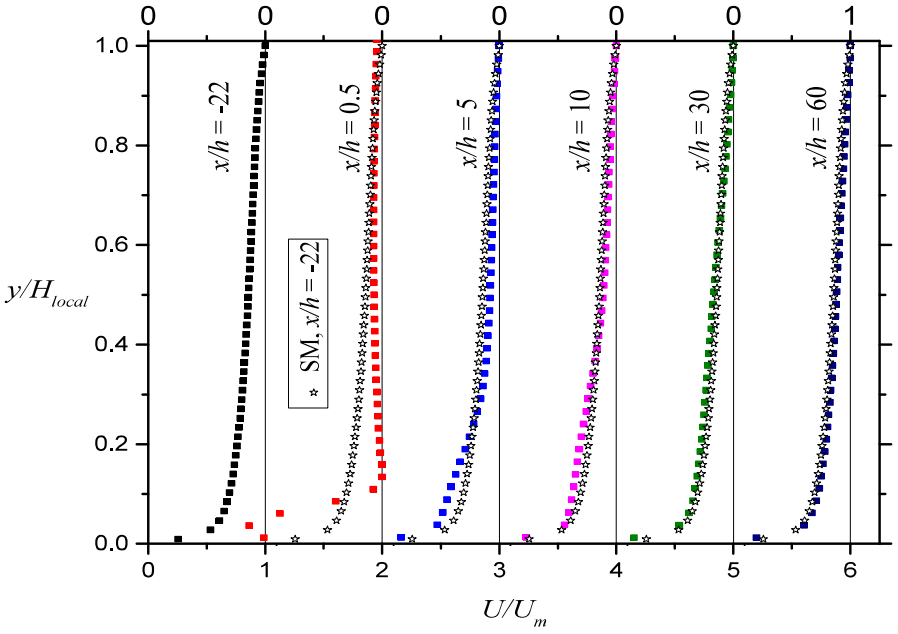

(a)

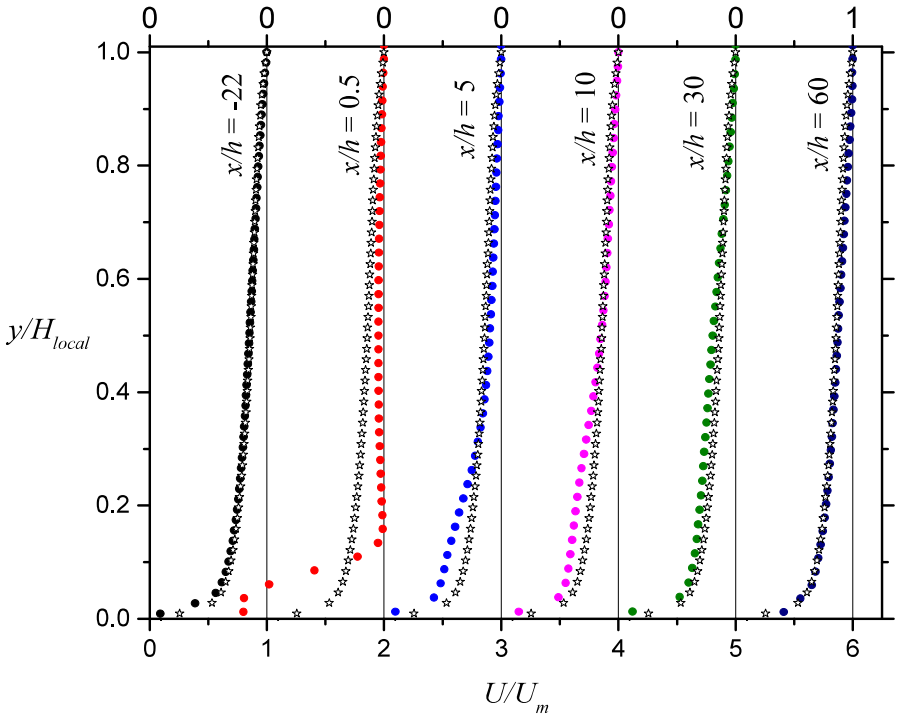

(b)

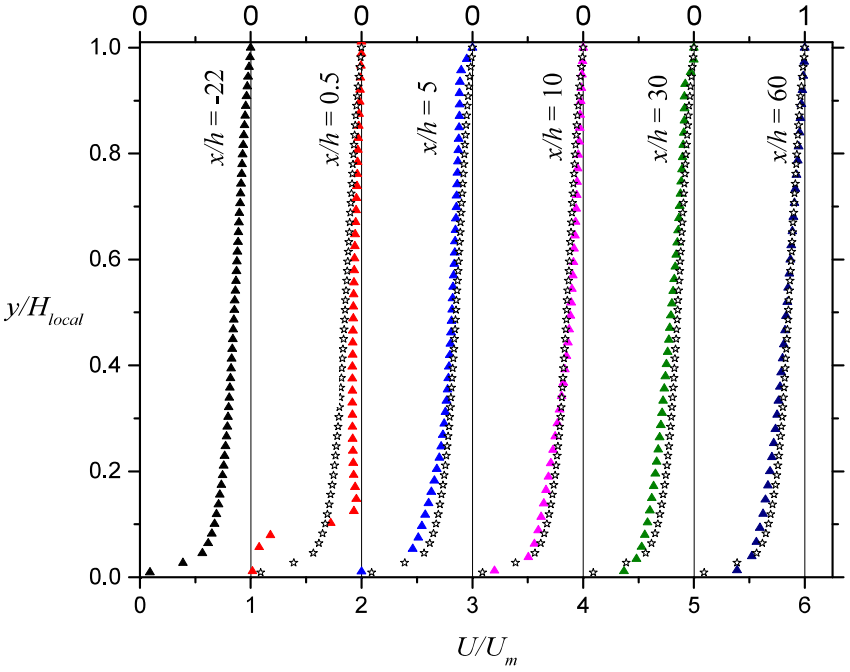

(c)

Fig. 6 Profiles of streamwise mean velocity for (a) SM-SM, (b) SP-SM and (c) SP-SP at different *x/h* locations with the corresponding smooth and rough upstream profiles

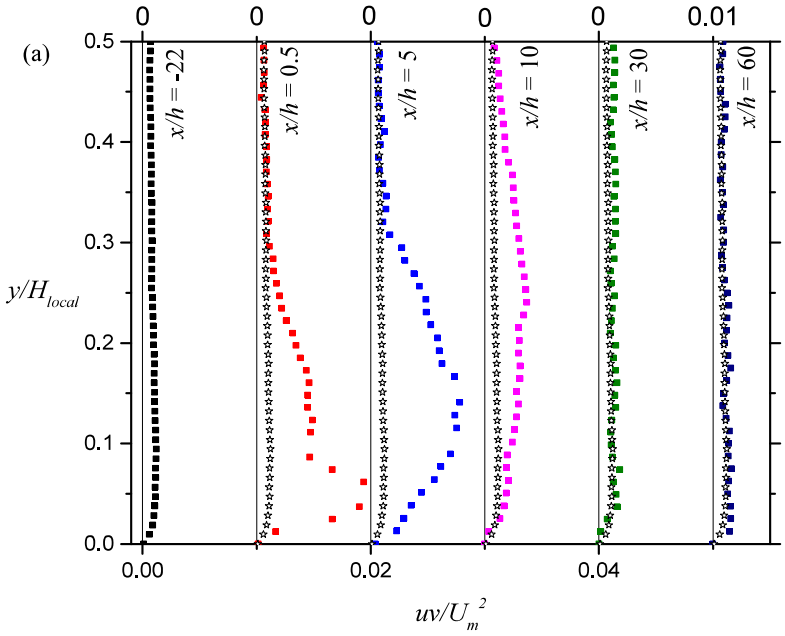

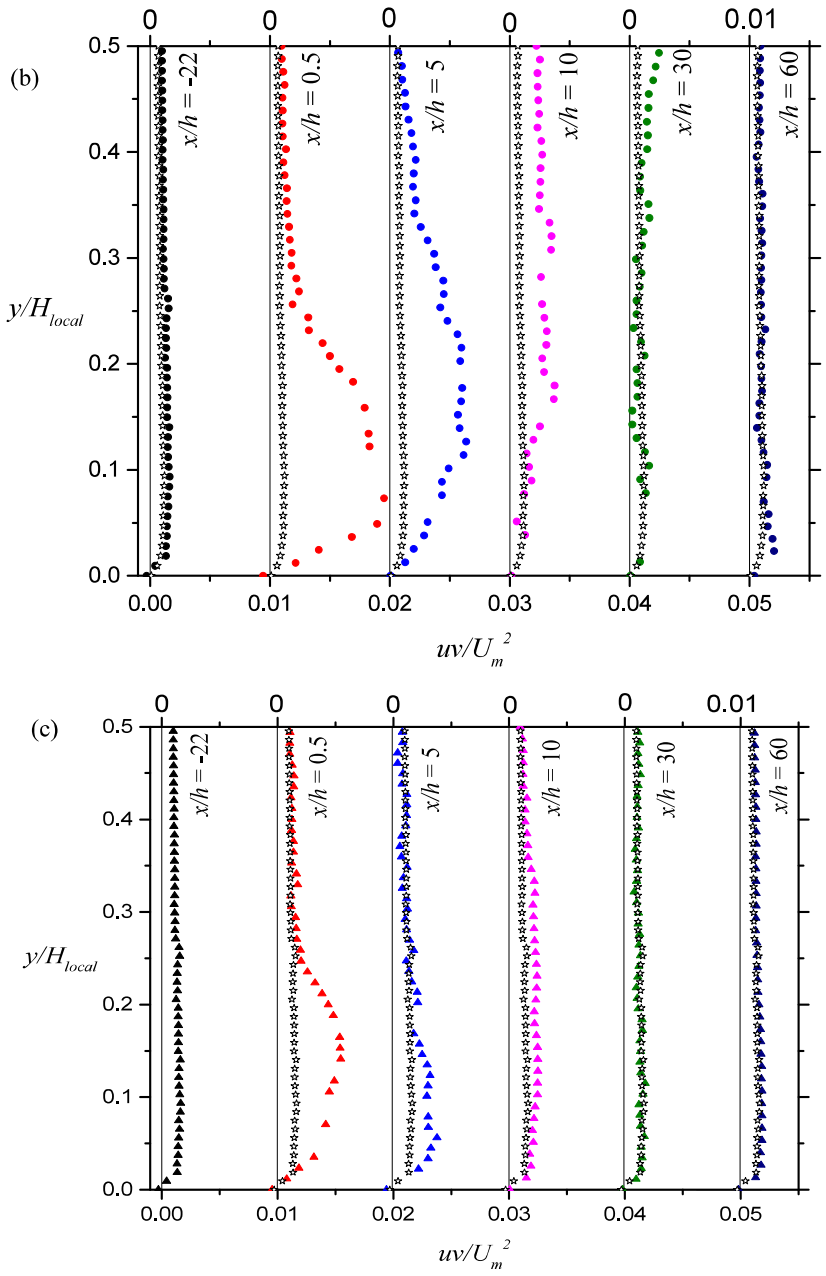

Fig. 7 Profiles of Reynolds shear stress for (a) SM-SM, (b) SP-SM and (c) SP-SP at different *x/h* locations with the corresponding smooth and rough upstream profiles

Figs. 7 and 8 show the profiles of Reynolds shear stress turbulent kinetic energy respectively at different *x/h* locations. For each wall condition, the maximum values of Reynolds shear stress and turbulent kinetic energy are significantly larger in the recirculation and early redevelopment regions than further downstream of the redevelopment region. Moreover, upstream roughness increases the peak values of Reynolds shear stress and turbulent kinetic energy but downstream roughness decreases the peak. For example, SP-SM case showed a 22% increase in the peak value of $<-u'v'>$ at $x/h = 0.5$ compared to the SM-SM case, but SP-SP showed a 39% reduction in the peak value. As for turbulent kinetic energy, SP-SM showed an increase of 13% and SP-SP showed a decrease of 19% of the peak values compared to the corresponding SM-SM value. However, for each wall condition, the peak values of Reynolds shear stress and turbulent kinetic energy in recirculation and early development regions are several times larger than their corresponding upstream values. The elevated Reynolds shear stress and turbulent kinetic energy in recirculation and early development regions is attributed to the presence of energetic large scale structures associated with a separated shear layer.

The reduced levels of Reynolds shear stress and turbulent kinetic energy in the redevelopment regions may be attributed to the mixing and spreading of the new boundary layer which cause a gradual breakdown of the large scale structures [12].

It is observed from the profiles that the Reynolds shear stress and turbulent kinetic energy recover slower than the streamwise mean velocity, but at x/h = 60 all the profiles are fairly similar to their corresponding upstream profiles. To obtain a complete collapse, several more streamwise distances would be required, which is also evident in the previous studies. For example, [4] observed the turbulence intensity profiles over a FFS to become self-similar for $x/h \geq 100$.

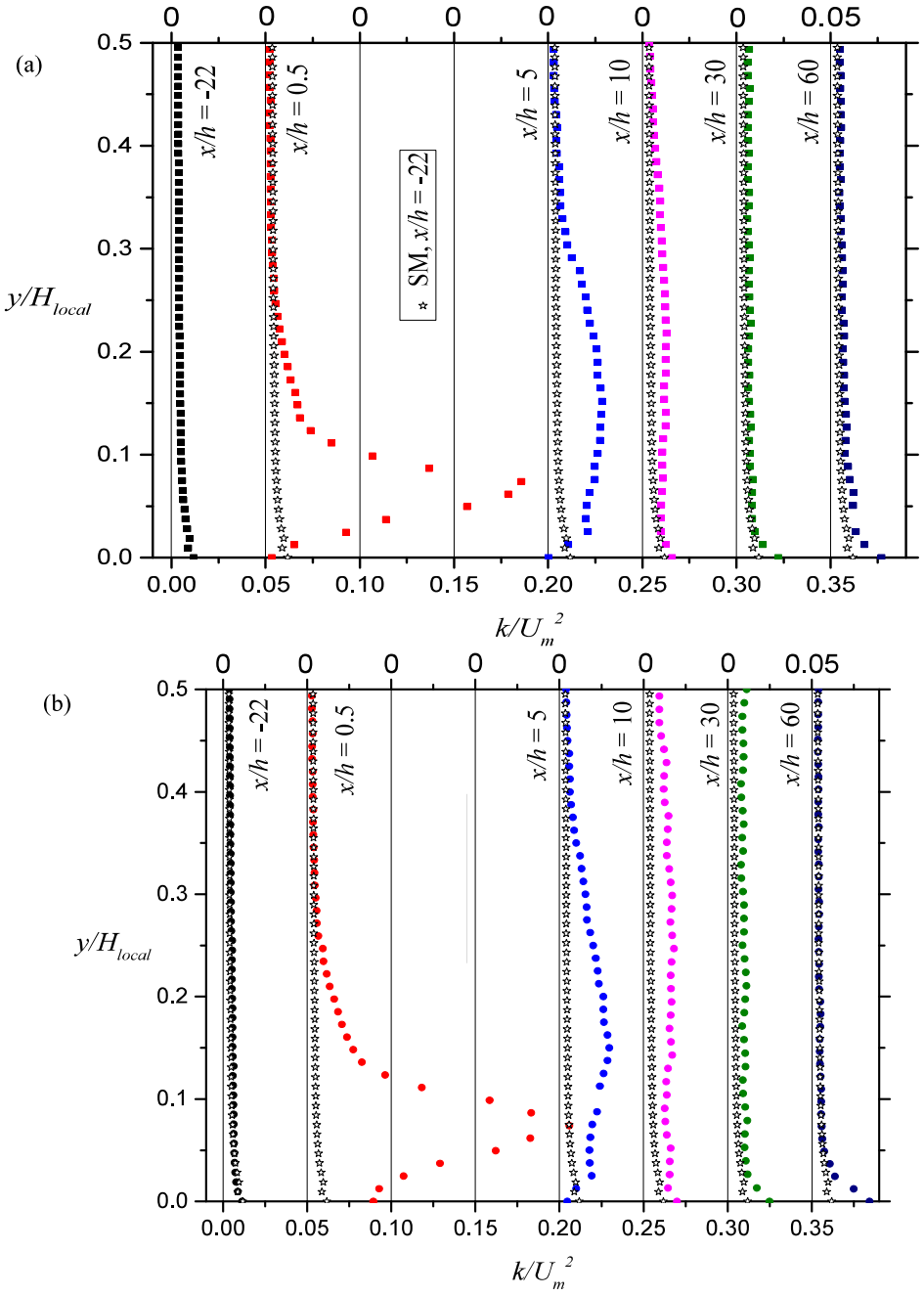

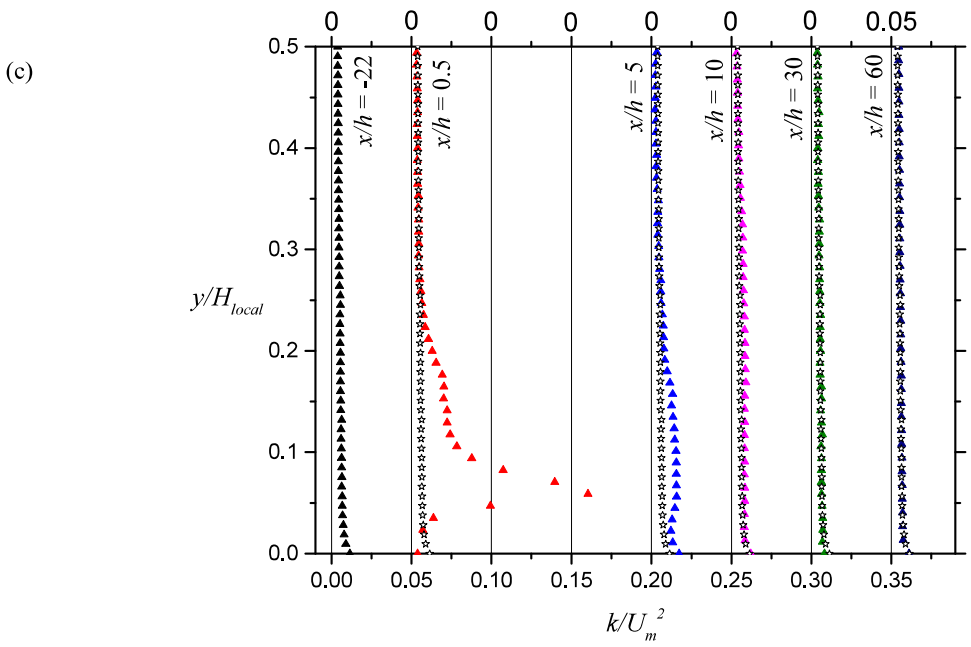

Fig. 8 Profiles of turbulent kinetic energy for (a) SM-SM, (b) SP-SM and (c) SP-SP at different x/h locations with the corresponding smooth and rough upstream profiles

C. Quadrant Decomposition

To investigate the dominant Reynolds shear stress producing events, quadrant decomposition of the streamwise and vertical fluctuating velocities was performed. Following the methodology from [13], the Reynolds shear stress was divided into four quadrants; outward interaction ($Q1$ events), ejections ($Q2$ events), inward interactions ($Q3$ events) and sweeps ($Q4$ events) using hyperbolic hole, $H = 0$. The value H represents a threshold on the strength of the Reynolds stress producing events considered in the analysis, with $H = 0$ allowing all events to be included in the decomposition and increasing values of H allowing inclusion of only increasingly strong Reynolds-stress-producing events. In this analysis, $H = 0$ was used. Fig. 9 shows the profiles of the quadrant analysis. As anticipated, the events in the second and fourth quadrants ($Q2$ and $Q4$) are dominant compared to the first and third quadrants ($Q3$ and $Q4$). When rough-wall contributions were compared with the smooth-wall baseline, excellent collapse was observed for all four quadrants after $y/h > 1$. Similar collapse was observed in the outer layer in quadrant analysis results of [14]. From Fig. 7 it is obvious that the upstream rough wall increased the peak values of the contributions of all four quadrants especially in the recirculation region ($x/h = 0.5$), although the rough surface on top of the step seems to diminish the peak values for all the quadrants. For example, compared to SM-SM at $x/h = 0.5$, the maximum negative peak was almost 30% higher and 18% lower for $Q1$ and 50% higher and 50% lower for $Q3$ respectively for SP-SM and SP-SP. On the other hand, for SP-SM, the maximum positive peak of $Q2$ and $Q4$ was 5% and 9% higher and for SP-SP, 12% and 10% lower compared to the SM-SM values.

IV. Concluding Remarks

An experimental study was conducted using particle image velocimetry technique to investigate the effects of upstream and downstream wall roughness on separated and reattached flow characteristics over a forward facing step in an open channel turbulent flow. Reference smooth upstream and downstream wall, rough upstream and smooth downstream wall and rough upstream and downstream wall were investigated in this paper. The rough wall was produced from sandpaper 36 grit. For each wall conditions, the Reynolds number, aspect ratio, blockage ratio and Froude number were kept constant to observe the effect of only wall roughness on the results. It was observed that upstream wall roughness increased momentum deficit and turbulence level. The maximum reduction of the reattachment length by upstream wall roughness was 14%. The downstream wall roughness diminished the recirculation bubbles and decreased most of the values which were already affected by the upstream roughness. The upstream wall roughness decreased the physical size of the contour levels of maximum positive Reynolds shear stress in the separated and reattached regions; the downstream wall roughness decreased it even more. Wall roughness has no significant effect on stream wise mean velocity away from the wall but reduced the velocity close to the wall. The one dimensional profiles showed the quantitative differences between the three test cases. The maximum backflow for SM-SM was 50% lower than the corresponding SP-SM value which may be an attribute of the higher drag produced by the upstream wall roughness. In the recirculation region, compared to their smooth wall counterparts, both Reynolds shear stress and turbulent kinetic energy increased for SP-SM and decreased for SP-SP, but these values are

several times larger than their upstream values. As we move downstream after the reattachment point, the peak values started to decrease and at $x/h = 60$, the values are fairly similar to the corresponding upstream values. Quadrant analysis was performed to investigate the dominant Reynolds shear stress contribution in the recirculation region. $Q2$ and $Q4$ events were found to be more dominant than the $Q1$ and $Q3$ events. Upstream roughness increased the maximum positive and negative peaks by almost 9% and 50%, but the downstream roughness decreased the maximum positive and negative peaks by almost 12% and 50% compared to the smooth wall.

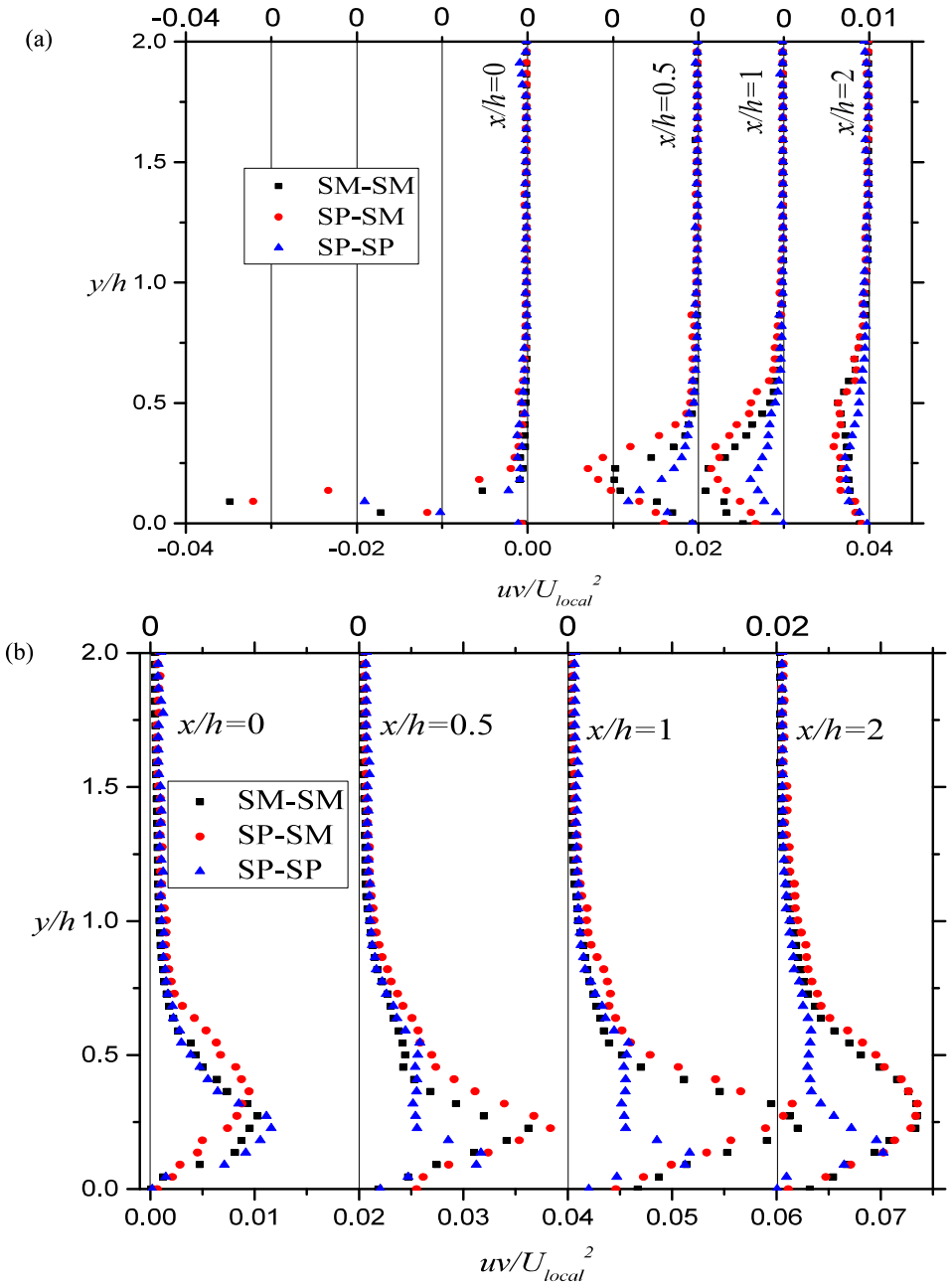

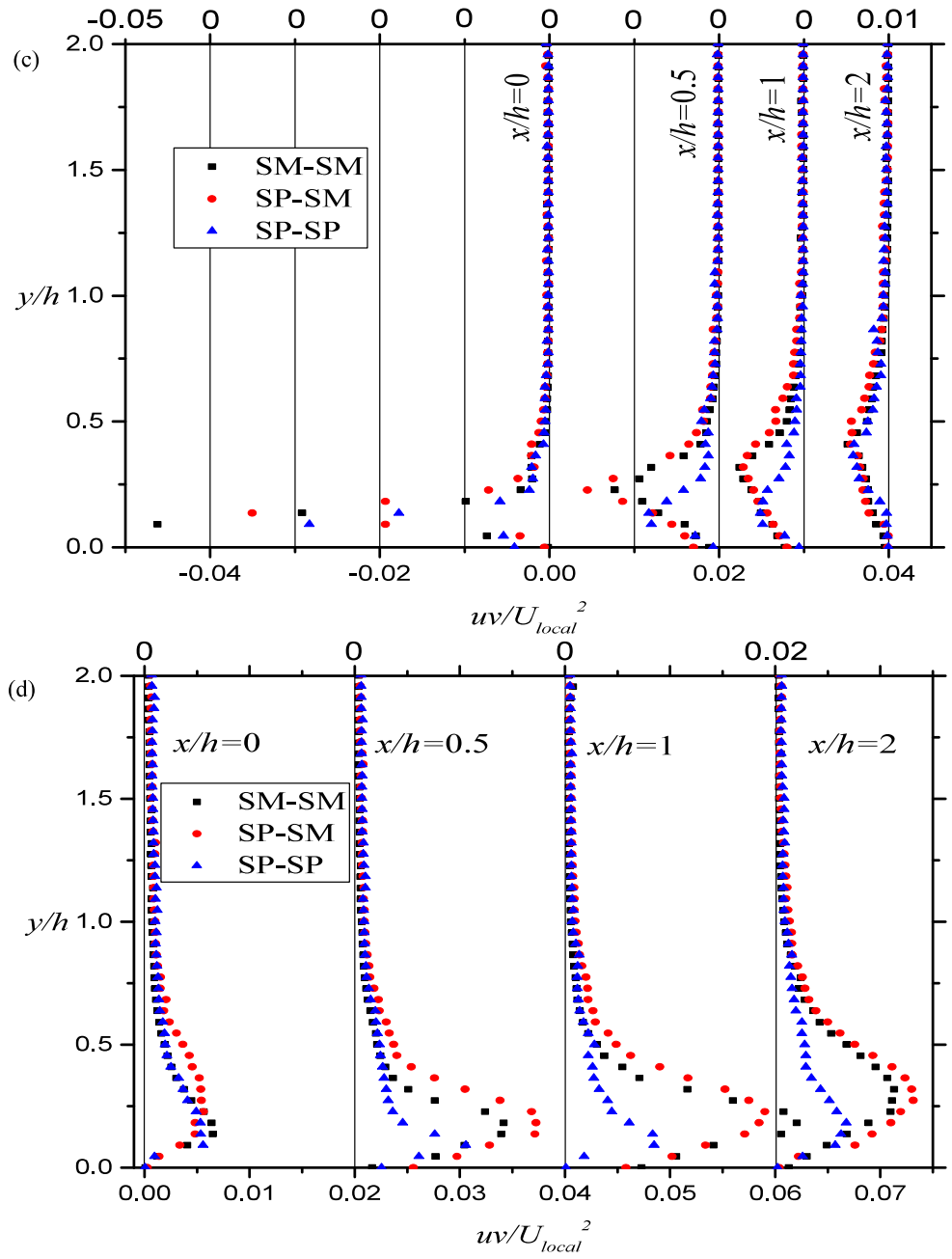

Fig. 9 Profiles of quadrant decomposition for (a) $Q1$, (b) $Q2$, (c) $Q3$ and (d) $Q4$ at different x/h locations at the vicinity of the leading edge of the step

ACKNOWLEDGMENT

The authors acknowledge the support of this work by the Natural Sciences and Engineering Research Council of Canada (NSERC).

REFERENCES

[1] H. Ren and Y. Wu, "Turbulent boundary layers over smooth and rough forward-facing steps," *Phys. Fluids*. 23 (2011), 045102.

[2] Y. Wu and H. Ren, "On the impacts of coarse-scale models of realistic roughness on a forward-facing step turbulent flow," *Int. J. Heat Fluid Flow*, Vol. 40, pp. 15–31.

[3] E. E. Essel, S. Mali, E. W. Thacher and M. F. Tachie, "Upstream roughness effects on reattached turbulent flow over forward facing step," *10th International ERCOFTAC Symposium on Engineering Turbulence Modelling and Measurements*, Spain, September 2014.

[4] M. F. Tachie, R. Balachandar and D. J. Bergstrom, "Open channel boundary layer relaxation behind a forward facing step at low Reynolds numbers," *Journal of Fluids Engineering*, Vol. 123, pp. 539-545, September 2001.

[5] M. Agelinchaab and M. F. Tachie, "PIV study of separated and reattached open channel flow over surface mounted blocks," *Journal of Fluids Engineering*, Vol. 130, pp. 061206-1-061206-9, June 2008.
[6] J. F. Largeau and V. Moriniere, "Wall pressure fluctuations and topology in separated flows over a forward-facing Step," *Exp. Fluids*, Vol. 42, pp. 21–40.
[7] V. De Brederode and P. Bradshaw, "Three-dimensional flow in nominally two-dimensional separation bubbles: flow behind a rearward-facing step," Imp. Coll. Aeronaut. Rep., pp. 72–19.
[8] K. A. Flack and M. P. Schultz, "Review of Hydraulic Roughness Scales in the Fully Rough Regime," *J. Fluids Eng*. 132, 041203–10.
[9] D. J. Forliti, P. J. Strykowski, and K. Debatin, "Bias and precision errors of digital particle image velocimetry," *Exp. Fluids*. 28 (2000), pp. 436–447.
[10] L. Casarsa and P. Giannattasio, "Three-dimensional features of the turbulent flow through a planar sudden expansion," *Phys. Fluids*. 20 (2008), 015103.
[11] E.E. Essel, A. Nematollahi, E.W. Thacher and M.F. Tachie, "Effects of upstream roughness and Reynolds number on separated and reattached turbulent flow," *Journal of Turbulence*, Vol. 16, Issue 9, 2015.
[12] P. Bradshaw and F. Y. F. Wong, "The reattachment and relaxation of a turbulent boundary layer," *J. Fluid Mech.,* Vol. 52, part 1, pp. 113-135, 1972.
[13] S. S. Lu and W. W. Willmarth, "Measurement of the structure of the Reynolds stress in a turbulent boundary layer," *J. Fluid Mech.*, Vol. 60(part 3), pp. 481–511, 1973.
[14] Y. Wu and K. T. Christensen, "Outer-layer similarity in the presence of a practical rough-wall topography," *Phys. Fluids* 19, 085108, 2007.